

# Multiscale modelling and computation of fluid flow

Thomas Y. Hou<sup>\*,†</sup>

*Applied and Computational Mathematics, 217-50, Caltech, Pasadena, CA 91125, U.S.A.*

## SUMMARY

Many problems of fundamental and practical importance have multiscale solutions. Direct numerical simulation of these multiscale problems is difficult due to the range of length scales in the underlying physical problems. Here, we describe two multiscale methods for computing nonlinear partial differential equations with multiscale solutions. The first method relies on constructing local multiscale bases for diffusion-dominated problems. We demonstrate that such an approach can be used to upscale two-phase flow in heterogeneous porous media. The second method is to construct semi-analytic multiscale solutions local in space and time. We use these solutions to approximate the large-scale solution for convection-dominated transport. This approach overcomes the common difficulty due to the memory effect in deriving the averaged equations for convection-dominated transport. Our multiscale analysis provides a useful guideline for designing effective numerical methods for incompressible flow. Copyright © 2005 John Wiley & Sons, Ltd.

KEY WORDS: multiscale computation; incompressible flow; upscaling; porous media

## 1. INTRODUCTION

Many physical problems have multiscale solutions. Examples include the behaviour of composite materials, wave propagation in random media, flow and transport through heterogeneous porous media, and turbulent flow. Accurately computing these multiscale solutions presents a challenge due to the wide range of length scales in the solutions. Resolving small-scale dynamics has been a bottleneck in computation. For engineering applications, it is desirable to develop a multiscale method that captures the large-scale solution accurately on a coarse grid, but does not require resolving the small-scale features. Such multiscale methods offer significant computational savings.

---

\*Correspondence to: Thomas Y. Hou, Applied and Computational Mathematics, 217-50, Caltech, Pasadena, CA 91125, U.S.A.

†E-mail: hou@ama.caltech.edu

Contract/grant sponsor: NSF; contract/grant number: ACI-0204932

*Received 27 April 2004*

*Revised 7 September 2004*

*Accepted 3 November 2004*

We use immiscible two-phase flow in heterogeneous porous media and incompressible flow as examples to illustrate some key issues in designing multiscale computational methods for fluid flows. Two-phase flows have many applications in oil reservoir simulations and environmental science problems. Through the use of sophisticated geological and geostatistical modelling tools, engineers and geologists can now generate highly detailed, three-dimensional representations of reservoir properties. The direct numerical simulation of these highly resolved models for reservoir simulation is not generally feasible because their fine level of detail (tens of millions grid blocks) places prohibitive demands on computational resources. Therefore, the ability to coarsen these highly resolved geologic models to levels of detail appropriate for reservoir simulation (tens of thousands grid blocks), while maintaining the integrity of the model for purpose of flow simulation, is clearly needed.

In recent years, we have introduced a multiscale finite element method (MsFEM) for solving partial differential equations with multiscale solutions [1–4]. The central goal of this approach is to obtain the large-scale solutions accurately and efficiently without resolving the small-scale details. The main idea is to construct finite element base functions which capture the small-scale information within each element. The small scale information is then brought to the large scales through the coupling of the global stiffness matrix. Thus, the effect of small scales on the large scales is correctly captured. In our method, the base functions are constructed from the leading order homogeneous elliptic equation in each element. As a consequence, the base functions are adapted to the local microstructure of the differential operator. In the case of two-scale periodic structures, we have proved that the multiscale method indeed converges to the correct solution independent of the small scale in the homogenization limit [2].

We remark that the idea of using base functions governed by the differential equations has been used elsewhere in the finite element community, see e.g. Reference [5]. The multiscale finite element method presented here is also similar in spirit to the residual-free bubble finite element method [6] and the variational multiscale method [7].

## 2. FORMULATION FOR TWO-PHASE FLOW

We consider the flow and transport problems in porous media in a hierarchy of approximation levels. At the microscale, solute transport is governed by the convection–diffusion equation in a homogeneous fluid. However, in the case of porous media, it is very difficult to obtain full information about the pore structure. An averaging procedure has to be carried out, and the porous medium becomes a continuum with certain macroscopic properties, such as the porosity and permeability. With modern geostatistical techniques, one can routinely generate a fine grid model as large as tens of millions of grid blocks. As a first step, we upscale the fine grid model to a coarse grid model consisting of tens of thousands of coarse grid blocks while preserving the integrity of the original fine grid model. Once the coarse grid model is obtained, it can be reapplied with different boundary conditions or source distributions as is typical in model validation and oil field management. This can reduce the computational cost significantly.

We consider a heterogeneous system which represents two-phase immiscible flow. Our interest is in the effect of permeability heterogeneity on the flow, so we neglect the effect of compressibility and capillary pressure. Also, we consider porosity to be constant. Each phase

obeys Darcy’s law

$$\mathbf{v}_j = \frac{k_{rj}(S)}{\mu_j} \mathcal{K}^\varepsilon \nabla p \tag{1}$$

For each phase  $j$ ,  $j = o, w$  for oil and water,  $\mathbf{v}_j$  is Darcy’s velocity,  $k_{rj}$  is the relative permeability, and  $\mu_j$  is the viscosity. In addition,  $p$  is pressure,  $S$  is water saturation,  $\mathcal{K}^\varepsilon$  is the permeability tensor, and  $\varepsilon$  represents the pore diameter. All quantities are dimensionless. Darcy’s law for each phase, coupled with mass conservation, can be manipulated to give the pressure and saturation equations as

$$\nabla \cdot (\lambda(S) \mathcal{K}^\varepsilon \nabla p) = 0 \tag{2}$$

$$\frac{\partial S}{\partial t} + \mathbf{u}^\varepsilon \cdot \nabla f(S) = 0 \tag{3}$$

where

$$\lambda(S) = \frac{k_{rw}(S)}{\mu_w} + \frac{k_{ro}(S)}{\mu_o}, \quad f(S) = \frac{k_{rw}(S)/\mu_w}{\lambda(S)}$$

are the total fluid mobility, and the relative water mobility, respectively. These equations can be solved subject to some appropriate initial and boundary conditions. The velocity field is given by  $\mathbf{u}^\varepsilon = \mathbf{v}_w + \mathbf{v}_o = -\lambda(S) \mathcal{K}^\varepsilon \nabla p$ .

We remark that the permeability tensor  $\mathcal{K}^\varepsilon$  in an oil reservoir model contains a continuous spectrum of scales that are not separable. The variation in the permeability tensor is also large, with the ratio between the maximum and minimum permeability being as great as  $10^6$ . See References [8, 9] for discussions on reservoir characterization in heterogeneous porous media. The high aspect ratio and the heterogeneity of the permeability field makes it very expensive to solve the pressure equation.

### 3. MULTISCALE FINITE ELEMENT METHOD

We first review the MsFEM for solving the pressure equation with highly oscillating coefficients. We consider the following elliptic problem:

$$L_\varepsilon u^\varepsilon := -\nabla \cdot (a^\varepsilon(\mathbf{x}) \nabla u^\varepsilon) = f \quad \text{in } \Omega, \quad u = 0 \quad \text{on } \partial\Omega \tag{4}$$

where  $a^\varepsilon(\mathbf{x}) = (a_{ij}^\varepsilon(\mathbf{x}))$  is a symmetric positive definite matrix,  $\Omega$  is the physical domain and  $\partial\Omega$  denotes the boundary of domain  $\Omega$ .

The main idea of the method is to construct finite element base functions which capture the small-scale information within each element. This is accomplished by requiring that the base functions satisfy the leading order homogeneous differential equation within each coarse grid element:

$$L_\varepsilon \phi^\varepsilon = 0, \quad x \in K$$

We need to specify boundary conditions for the multiscale base function within each element  $K$  in order to solve it locally. The simplest choice of the boundary condition for the base

function is a linear boundary condition, and we discuss this choice below. The MsFEM is the Galerkin finite element method with the finite element solution space spanned by the multiscale bases given above. When the coefficient  $a^\varepsilon$  has a two-scale periodic structure, i.e.  $a^\varepsilon(\mathbf{x}) = a(\mathbf{x}, \mathbf{x}/\varepsilon)$  with  $a(\mathbf{x}, \mathbf{y})$  being periodic in  $\mathbf{y}$ , we can show that the MsFEM gives a convergent result uniform in  $\varepsilon$  as  $\varepsilon$  tends to zero [2].

*Theorem 3.1*

Let  $u^\varepsilon \in H^2(\Omega)$  be the solution of (4) and  $u_h$  be the finite element solution obtained from the space spanned by the multiscale bases,  $\phi^\varepsilon$ . Then we have

$$\|u^\varepsilon - u_h\|_{H^1} \leq C(h + \varepsilon)\|f\|_{L^2} + C\left(\frac{\varepsilon}{h}\right)^{1/2}\|u_0\|_{H^2} \quad (5)$$

where  $u_0 \in H^2(\Omega) \cap W^{1,\infty}(\Omega)$  is the solution of the homogenized equation.

*3.1. Over-sampling*

As we can see from the above theorem, the MsFEM gives the correct homogenized result as  $\varepsilon$  tends to zero. In contrast, the error in the traditional FEM grows like  $O(h^2/\varepsilon^2)$  as  $\varepsilon \rightarrow 0$ . On the other hand, we also observe that when  $h \sim \varepsilon$ , the multiscale method attains large error in both  $H^1$  and  $L^2$  norms. This is what we call the *resonance* effect between the grid scale ( $h$ ) and the small scale ( $\varepsilon$ ) of the problem. We shall illustrate resonance in a specific case, and propose a general *over-sampling* method to address the effect.

The resonance effect can be seen, for example, where scale separation is possible for a periodic microstructure. Using standard homogenization theory [10], we can perform a multiscale expansion for the base function,  $\phi^\varepsilon(\mathbf{x}, \mathbf{y})$ , with  $\mathbf{y} = \mathbf{x}/\varepsilon$ :

$$\phi^\varepsilon = \phi_0(\mathbf{x}) + \varepsilon\phi_1(\mathbf{x}, \mathbf{y}) + \varepsilon\theta^\varepsilon(\mathbf{x}) + O(\varepsilon^2)$$

where  $\phi_0$  is the linear finite element base and  $\phi_1$  is the first-order corrector. The boundary corrector  $\theta^\varepsilon$  is chosen so that the boundary condition of  $\phi^\varepsilon$  on  $\partial K$  is exactly satisfied by the first three terms in the expansion. By solving a periodic cell problem for  $\chi^j$ ,

$$\nabla_{\mathbf{y}} \cdot a(\mathbf{x}, \mathbf{y}) \nabla_{\mathbf{y}} \chi^j = \frac{\partial}{\partial y_i} a_{ij}(\mathbf{x}, \mathbf{y}) \quad (6)$$

where  $\chi^j$  has zero mean, we can express the first-order corrector as  $\phi_1(\mathbf{x}, \mathbf{y}) = -\chi^j \partial \phi_0 / \partial x_j$ . The boundary corrector,  $\theta^\varepsilon$ , then satisfies

$$\nabla_{\mathbf{x}} \cdot a(\mathbf{x}, \mathbf{x}/\varepsilon) \nabla_{\mathbf{x}} \theta^\varepsilon = 0 \quad \text{in } K$$

with boundary condition  $\theta^\varepsilon|_{\partial K} = \phi_1(\mathbf{x}, \mathbf{x}/\varepsilon)|_{\partial K}$ .

The oscillatory boundary condition of  $\theta^\varepsilon$  introduces a numerical boundary layer, which leads to the so-called resonance error [1]. To avoid this resonance error, we need to incorporate the multi-dimensional oscillatory information through the cell problem into our boundary condition for  $\phi^\varepsilon$ . If we set  $\phi^\varepsilon|_{\partial K} = (\phi_0 + \varepsilon\phi_1(\mathbf{x}, \mathbf{x}/\varepsilon))|_{\partial K}$ , then the boundary condition for  $\theta^\varepsilon|_{\partial K}$  becomes identically equal to zero. Therefore, we have  $\theta^\varepsilon \equiv 0$ . In this case, we have an analytic expression for the multiscale base functions  $\phi^\varepsilon$  as follows:

$$\phi^\varepsilon = \phi_0(\mathbf{x}) + \varepsilon\phi_1(\mathbf{x}, \mathbf{x}/\varepsilon) \quad (7)$$

This set of multiscale bases avoids the boundary layer effect completely and can be computed efficiently, see [www.ama.caltech.edu/~westhead/MSFEM](http://www.ama.caltech.edu/~westhead/MSFEM) for numerical examples. For its linear boundary condition, we refer to this as a linear multiscale FEM, or MsFEM-L.

Unfortunately, for problems that do not have scale separation and periodic microstructure, we cannot use this approach to compute the multiscale base functions. Our convergence analysis motivates an over-sampling method to overcome the difficulty due to scale resonance [1]. The idea is quite simple and easy to implement. Since the boundary layer in the first-order corrector is thin,  $O(\varepsilon)$ , we can sample in a domain with size larger than  $h + \varepsilon$  and use only the interior sampled information to construct the bases. By doing this, we can reduce the influence of the boundary layer in the larger sample domain on the base functions significantly. As a consequence, we obtain an improved rate of convergence.

### 3.2. Accuracy and recovery of a small-scale solution

To assess the accuracy of our over-sampling method, we compare MsFEM with a traditional linear finite element method (LFEM) using a subgrid mesh,  $h_s = h/M$ . The multiscale bases are computed using the same subgrid mesh. Note that MsFEM only captures the solution at the coarse grid  $h$ , while FEM tries to resolve the solution at the fine grid  $h_s$ . Our extensive numerical experiments demonstrate that the accuracy of MsFEM on the coarse grid  $h$  is comparable to that of the corresponding highly resolved LFEM calculation at the same coarse grid. In some cases, MsFEM gives even more accurate results than LFEM.

We illustrate the convergence of the MsFEM for the case when the coefficient is random and has no scale separation nor periodic structure. In Figure 1, we show the results for a log-normally distributed  $a^\varepsilon$ . In this case, the effect of scale resonance shows clearly for MsFEM-L, i.e., the error increases as  $h$  approaches  $\varepsilon$ . Here  $\varepsilon \sim 0.004$  roughly equals the correlation length,  $h$ . Even the use of an oscillatory boundary condition (MsFEM-O), which is obtained by solving a reduced 1-D problem along the edge of the element [1], does not help much in this case. On the other hand, MsFEM with over-sampling agrees well with the highly resolved calculation.

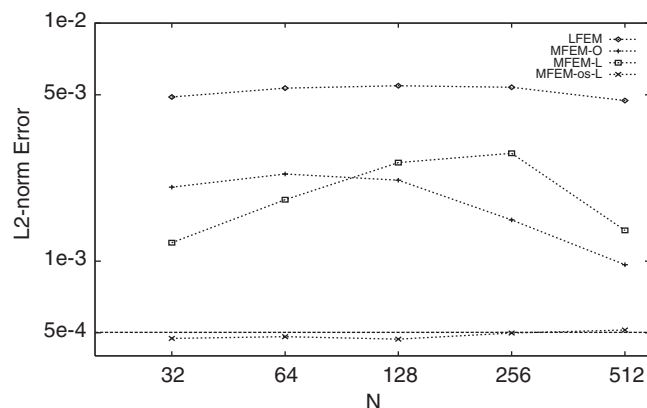


Figure 1. The  $l^2$ -norm error of the solutions using various schemes for a log-normally distributed permeability field. All solutions are compared to a fine LFEM calculation.

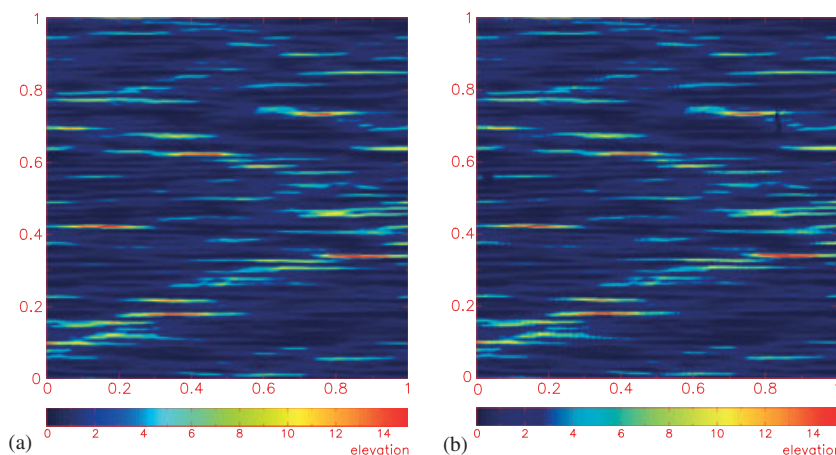


Figure 2. (a) Fine grid horizontal velocity field,  $N = 1024$ ; and (b) Recovered horizontal velocity field from the coarse grid calculation ( $N = 64$ ) using multiscale bases.

To solve the transport equation in the two-phase flows, we need to compute the velocity field from the elliptic equation for pressure, i.e.  $\mathbf{u}^\varepsilon = -\lambda(S)\mathcal{K}^\varepsilon \nabla p$ . For MsFEM, the fine scale velocity can be easily recovered from the multiscale base functions, which provide interpolations from the coarse  $h$ -grid to the fine  $h_s$ -grid. To illustrate that we can recover the fine grid velocity field from the coarse grid pressure calculation, we use a layered random medium. We compare the computations of the horizontal velocity fields obtained by two methods. In Figure 2(a), we plot the horizontal velocity field obtained by using a fine grid ( $N = 1024$ ) calculation. In Figure 2(b), we plot the same horizontal velocity obtained by using the coarse grid ( $N = 64$ ) pressure calculation and using the multiscale bases to interpolate the fine grid velocity. We can see that the recovered velocity field captures the layer structure in the fine grid velocity field. Further, we use the recovered fine grid velocity field to compute the saturation on a fine grid in time. In Figure 3(a), we plot the saturation at  $t = 0.06$  obtained by the fine grid calculation. Figure 3(b) shows the corresponding saturation obtained using the recovered velocity field from the coarse grid calculation. Most of detailed fine scale fingering structures in the well-resolved saturation are captured by the corresponding calculation using the recovered velocity field from the coarse grid pressure calculation. The agreement is quite striking.

### 3.3. Upscaling the two-phase transport equation

The MsFEM can also be used to upscale the transport equation. Upscaling the convection-dominated transport is difficult due to the nonlocal history-dependent memory effect [11]. Here we use the upscaling method proposed in Reference [12] to design an overall coarse grid model for the transport equation. The work of Efendiev *et al.* [12] for upscaling the saturation equation involves a moment closure argument. The velocity and the saturation are separated into a local mean quantity  $\mathbf{u}_0$  and a small-scale perturbation  $\mathbf{u}'$  with zero mean. If we ignore the third-order terms containing the fluctuations of velocity and saturation, we

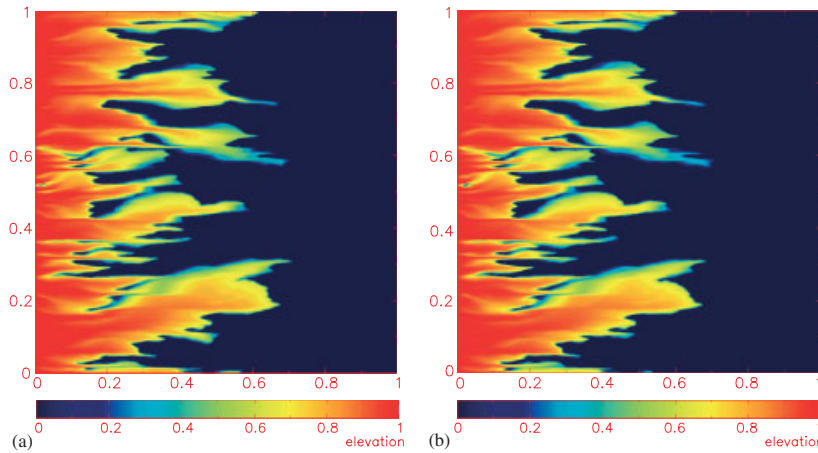


Figure 3. (a) Fine grid saturation at  $t = 0.06$ ,  $N = 1024$ ; and (b) Saturation computed using the recovered velocity field from the coarse grid calculation ( $N = 64$ ) using multiscale bases.

obtain an average equation for the saturation  $S$  as follows:

$$\frac{\partial S}{\partial t} + \mathbf{u}_0 \cdot \nabla f(S) = \nabla \cdot (f'(S)^2 D(\mathbf{x}, t) \nabla S) \tag{8}$$

where the diffusion coefficients  $D_{ij}(\mathbf{x}, t)$  are defined by

$$D_{ij}(\mathbf{x}, t) = \int_0^t \langle \mathbf{u}'_i(\mathbf{x}) \mathbf{u}'_j(\mathbf{y}(\tau)) \rangle d\tau$$

$\langle g \rangle$  denotes the average of  $g$  over each coarse element, and  $\mathbf{y}(s)$  is the solution of the following system of ODEs:

$$\frac{d\mathbf{y}(s)}{ds} = \mathbf{u}_0(\mathbf{y}(s)), \quad \mathbf{y}(t) = \mathbf{x}$$

Note that the upscaled equation for  $S$  is of a different type now, changing from the original convection equation to a convection–diffusion equation. Moreover, the enhanced diffusion coefficient is history dependent, reflecting the nonlocal memory effect inherent in upscaling convection-dominated transport [11]. The local fine grid velocity  $\mathbf{u}'$  can be reconstructed from the multiscale finite element bases. We perform a coarse grid computation of the above algorithm for the one-phase flow  $f(S) = S$  on the coarse  $64 \times 64$  mesh using a mixed MsFEM [4]. The fractional flow at the right boundary, defined as  $F = \int S u_1^e dy / \int u_1^e dy$ , where  $u_1^e$  is the horizontal velocity component, is shown in Figure 4. It gives excellent agreement with the reference fractional flow curve which is obtained using a fine  $1024 \times 1024$  mesh.

Upscaling the two-phase flow is difficult due to the dynamic coupling between the pressure and the saturation. One important observation is that the fluctuation in saturation is relatively small away from the oil/water interface. In this region, the multiscale bases are essentially the same as those generated by the corresponding one-phase flow (i.e.  $\lambda = 1$ ). These base functions are time independent. In practice, we can design an adaptive strategy to update

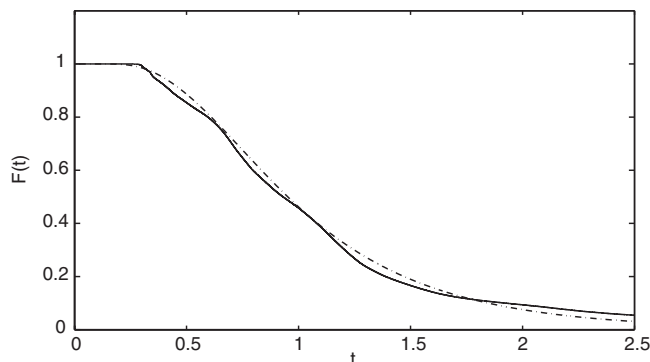


Figure 4. The accuracy of the coarse grid algorithm. The solid line is the well-resolved fractional flow curve. The slash-dotted line is the fractional flow curve using above coarse grid algorithm.

the multiscale bases in space and time. The percentage of multiscale bases that need to be updated is relatively small, typically a few percent of the total number of the bases [13]. The base functions that need to be updated are primarily those near the oil–water interface. For those coarse grid cells far from the interface, there is little dynamic change in mobility. Upscaling the saturation equation based on the moment closure argument can be generalized to two-phase flow with the enhanced diffusivity depending on the local small-scale velocity field [12]. As previously mentioned, fluctuation of the velocity field  $\mathbf{u}'$  can be accurately recovered from the coarse grid computation by using local multiscale bases.

Upscaling based on the moment closure argument is not easy to justify theoretically. In particular, the fluctuation of the velocity field  $\mathbf{u}'$  can be quite large in practice. Recently, we have developed a novel multiscale analysis for the convection-dominated transport equation [14]. An interesting feature of this analysis is that the fast variable,  $\mathbf{y} = \mathbf{x}/\varepsilon$ , which characterizes the small-scale solution, enters only as a parameter. This makes it easier for us to generalize our analysis to problems which do not have scale separation.

Other approaches to multiscale convection–diffusion problems have been developed, see e.g. References [15–19]. Some of these methods assume that the media have periodic microstructures or scale separation, and explore these properties in their multiscale methods, while others use wavelet approximations, renormalization group techniques, and variational methods.

#### 4. MULTISCALE ANALYSIS FOR INCOMPRESSIBLE FLOW

Upscaling the nonlinear transport equation in two-phase flows shares some of the common difficulties in deriving the effective equations for incompressible flow at high Reynolds number. Understanding scale interactions for 3-D incompressible flow has been a challenge. For high Reynolds number flow, the degrees of freedom are so numerous that it is almost impossible to resolve the flow all small-scales by direct numerical simulations. Deriving an effective equation for the large-scale solution is very useful in engineering applications, see e.g. References [20, 21]. In deriving a large eddy simulation model, one usually needs to make certain closure

assumptions. The accuracy of such closure models is hard to measure *a priori*, and varies from application to application. For many engineering applications, it is desirable to design a subgrid-based large-scale model in a systematic way so that we can measure and control the modelling error. However, the strong nonlinear interaction of small scales and the lack of scale separation make it difficult to derive an effective equation.

We consider the incompressible Navier–Stokes equation

$$\mathbf{u}_t^\varepsilon + (\mathbf{u}^\varepsilon \cdot \nabla) \mathbf{u}^\varepsilon = -\nabla p^\varepsilon + \nu \Delta \mathbf{u}^\varepsilon \tag{9}$$

$$\nabla \cdot \mathbf{u}^\varepsilon = 0 \tag{10}$$

with multiscale initial data  $\mathbf{u}^\varepsilon(\mathbf{x}, 0) = \mathbf{u}_0^\varepsilon(\mathbf{x})$ . Here  $\mathbf{u}^\varepsilon(t, \mathbf{x})$  and  $p^\varepsilon(t, \mathbf{x})$  are velocity and pressure, respectively.  $\nu$  is viscosity. The choice for  $\varepsilon$  is discussed below. We use boldface letters to denote vector variables. For the time being, we do not consider boundary effects, but assume that the solution is periodic with period  $2\pi$  in each dimension.

For incompressible flow at high Reynolds number, small scales are generated dynamically through nonlinear interactions. In general, there is no scale separation in the solution. However, by decomposing the physical solution into a lower frequency component and a high-frequency component, we can formally express the solution as the sum of a large-scale solution and a small-scale component. This decomposition can be carried out easily in Fourier space. Further, by rearranging the order of summation in the Fourier transformation, we can express the initial condition in the following form:

$$\mathbf{u}^\varepsilon(\mathbf{x}, 0) = \mathbf{U}(\mathbf{x}) + \mathbf{W}\left(\mathbf{x}, \frac{\mathbf{x}}{\varepsilon}\right)$$

where  $\mathbf{W}(\mathbf{x}, \mathbf{y})$  is periodic in  $\mathbf{y}$  and has mean zero. Here  $\varepsilon$  represents the cut-off wavelength in the solution above which the solution is resolvable and below which the solution is unresolvable. We call this a reparameterization technique. The question of interest is how to derive a homogenized equation for the averaged velocity field for small but finite  $\varepsilon$ .

If the problem is diffusion dominated, the small-scale solution will be damped out quickly in time. In order for the oscillatory component of the velocity field to persist in time, we need to have  $\nu = O(\varepsilon^2)$ . In this case, the cell viscosity is zero to the leading order. Since we are interested in the convection-dominated transport, we set  $\nu = 0$  and consider only the incompressible Euler equation.

The homogenization of the Euler equation with oscillating data was first studied by McLaughlin–Papanicolaou–Pironneau (MPP) [22]. In Reference [22], MPP made the important assumption that the small-scale oscillation is convected by the mean flow. Based on this assumption, they made the following multiscale expansion for velocity and pressure:

$$\mathbf{u}^\varepsilon(t, \mathbf{x}) = \mathbf{u}(t, \mathbf{x}) + \mathbf{w}\left(t, \mathbf{x}, \frac{t}{\varepsilon}, \frac{\boldsymbol{\theta}(t, \mathbf{x})}{\varepsilon}\right) + \varepsilon \mathbf{u}_1\left(t, \mathbf{x}, \frac{t}{\varepsilon}, \frac{\boldsymbol{\theta}(t, \mathbf{x})}{\varepsilon}\right) + \dots$$

$$p^\varepsilon(t, \mathbf{x}) = p(t, \mathbf{x}) + q\left(t, \mathbf{x}, \frac{t}{\varepsilon}, \frac{\boldsymbol{\theta}(t, \mathbf{x})}{\varepsilon}\right) + \varepsilon p_1\left(t, \mathbf{x}, \frac{t}{\varepsilon}, \frac{\boldsymbol{\theta}(t, \mathbf{x})}{\varepsilon}\right) + \dots$$

where  $\mathbf{w}(t, \mathbf{x}, \tau, \mathbf{y})$ ,  $\mathbf{u}_1(t, \mathbf{x}, \tau, \mathbf{y})$ ,  $q$ , and  $p_1$  are assumed to be periodic in both  $\mathbf{y}$  and  $\tau$ , and the phase  $\theta$  is convected by the mean velocity field  $\mathbf{u}$

$$\frac{\partial \theta}{\partial t} + \mathbf{u} \cdot \nabla_{\mathbf{x}} \theta = 0, \quad \theta(0, \mathbf{x}) = \mathbf{x} \quad (11)$$

By substituting the above multiscale expansions into the Euler equation and equating coefficients of the same order, MPP obtained a homogenized equation for  $(\mathbf{u}, p)$ , and a periodic cell problem for  $(\mathbf{w}(t, \mathbf{x}, \tau, \mathbf{y}), q(t, \mathbf{x}, \tau, \mathbf{y}))$ . On the other hand, it is not clear whether the resulting cell problem for  $\mathbf{w}$  and  $q$  has a unique solution that is periodic in both  $\mathbf{y}$  and  $\tau$ . Additional assumptions were imposed on the solution of the cell problem in order to derive a variant of the  $k - \varepsilon$  model.

Understanding how small-scale solutions propagate is clearly very important in deriving the homogenized equation. Motivated by the work of MPP, we have recently developed a multiscale analysis for the incompressible Euler equation with multiscale solutions [23]. Our study shows that the small-scale oscillations are convected by the full oscillatory velocity field, not just the mean velocity:

$$\frac{\partial \theta^\varepsilon}{\partial t} + \mathbf{u}^\varepsilon \cdot \nabla_{\mathbf{x}} \theta^\varepsilon = 0, \quad \theta^\varepsilon(0, \mathbf{x}) = \mathbf{x} \quad (12)$$

This is clear for the 2-D Euler equation since vorticity,  $\omega^\varepsilon$ , is conserved along the characteristics. That is

$$\omega^\varepsilon(t, \mathbf{x}) = \omega_0 \left( \theta^\varepsilon(t, \mathbf{x}), \frac{\theta^\varepsilon(t, \mathbf{x})}{\varepsilon} \right)$$

where  $\omega_0(\mathbf{x}, \mathbf{x}/\varepsilon)$  is the initial vorticity, which is of order  $O(1/\varepsilon)$ . A similar conclusion can be drawn for the 3-D Euler equation. Now the multiscale structure of  $\theta^\varepsilon(\mathbf{x}, t)$  is coupled to the multiscale structure of the flow. It is quite a challenge to unfold the multiscale solution structure. Naive multiscale expansion for  $\theta^\varepsilon$  may lead to generation of infinite number of scales.

Motivated by the above analysis, we look for multiscale expansions of the velocity field and the pressure of the following form:

$$\mathbf{u}^\varepsilon(t, \mathbf{x}) = \mathbf{u}(t, \mathbf{x}) + \mathbf{w}(t, \theta(t, \mathbf{x}), \tau, \mathbf{y}) + \varepsilon \mathbf{u}^{(1)}(t, \theta(t, \mathbf{x}), \tau, \mathbf{y}) + \dots \quad (13)$$

$$p^\varepsilon(t, \mathbf{x}) = p(t, \mathbf{x}) + q(t, \theta(t, \mathbf{x}), \tau, \mathbf{y}) + \varepsilon p^{(1)}(t, \theta(t, \mathbf{x}), \tau, \mathbf{y}) + \dots \quad (14)$$

where  $\tau = t/\varepsilon$  and  $\mathbf{y} = \theta^\varepsilon(t, \mathbf{x})/\varepsilon$ . We assume that  $\mathbf{w}$  and  $q$  have zero mean with respect to  $\mathbf{y}$ . The phase function  $\theta^\varepsilon$  is defined in (12) and it has the following multiscale expansion:

$$\theta^\varepsilon = \theta(t, \mathbf{x}) + \varepsilon \theta^{(1)} \left( t, \theta(t, \mathbf{x}), \tau, \frac{\theta^\varepsilon}{\varepsilon} \right) + \dots \quad (15)$$

This particular form of multiscale expansion is suggested by a corresponding Lagrangian multiscale analysis [23]. If one tried to expand  $\theta^\varepsilon$  naively as a function of  $\mathbf{x}/\varepsilon$  and  $t/\varepsilon$ , one would find that there is a generation of infinite number of scales at  $t > 0$  and would not be able to obtain a well-posed cell problem.

Expanding the Jacobian matrix, we get  $\nabla_x \theta^\varepsilon = \mathcal{B}^{(0)} + \varepsilon \mathcal{B}^{(1)} + \dots$ . Substituting the expansion into the Euler equation and matching the terms of the same order, we obtain the homogenized equation

$$\partial_t \mathbf{u} + \mathbf{u} \cdot \nabla_x \mathbf{u} + \nabla_x \cdot \langle \mathbf{w}\mathbf{w} \rangle = -\nabla_x p, \quad \mathbf{u}|_{t=0} = \mathbf{U}(\mathbf{x}) \tag{16}$$

$$\nabla_x \cdot \mathbf{u} = 0 \tag{17}$$

$\langle \mathbf{w}\mathbf{w} \rangle$ , the Reynolds stress term, is space-time average in  $(\mathbf{y}, \tau)$ , and  $\mathbf{w}\mathbf{w}$  is the matrix whose entry at the  $i$ th row and  $j$ th column is  $w_i w_j$ .  $\mathbf{w}$  is given by

$$\partial_\tau \mathbf{w} + \mathcal{B}^{(0)\top} \nabla_y q = 0, \quad \tau > 0 \tag{18}$$

$$(\mathcal{B}^{(0)\top} \nabla_y) \cdot \mathbf{w} = 0, \quad \mathbf{w}|_{\tau=0} = \mathbf{W}(\mathbf{x}, \mathbf{y}), \quad t = 0 \tag{19}$$

It can be shown that  $\mathcal{B}^{(0)\top} \nabla_y q$  has zero mean in  $\mathbf{y}$ . Note that there is no convection term in the equation for  $\mathbf{w}$  since we have treated convection at small scales exactly via the multiscale phase function. The equation for  $\mathbf{w}$  enforces incompressibility at small scales.

Finally, we compute  $\mathcal{B}^{(0)}$ .  $\theta$  and  $\theta^{(1)}$  obey the evolution equations

$$\partial_t \theta + (\mathbf{u} \cdot \nabla_x) \theta = 0, \quad \theta|_{t=0} = \mathbf{x} \tag{20}$$

$$\partial_\tau \theta^{(1)} + (\mathbf{w} \cdot \nabla_x) \theta^{(1)} = 0, \quad \theta^{(1)}|_{\tau=0} = 0 \tag{21}$$

and the Jacobian matrix is

$$\mathcal{B}^{(0)} = (I - D_y \theta^{(1)})^{-1} \nabla_x \theta \tag{22}$$

The above analysis can be extended to problems with general multiscale initial data without scale separation and periodic structure. This can be done by using the reparameterization technique in Fourier space, which we described earlier for the initial velocity. This reparameterization technique can be used repeatedly in time. The dynamic reparameterization also accounts for the dynamic interactions between the large and small scales. The difficulty associated with finding the local microscopic boundary condition can be overcome. Preliminary computational results show that the multiscale method can capture accurately the large-scale solution and the spectral properties of the small-scale solution.

Our goal is to use the multiscale analysis to design an effective coarse grid model that can capture accurately the large-scale behaviour but with a computational cost comparable to the traditional large eddy simulation (LES) models [20, 21]. To achieve this, we need to take into account the special structures in the fully mixed flow, such as homogeneity and possible local self-similarity of the flow in the interior of the domain. When the flow is fully mixed, we expect that the Reynolds stress term,  $\langle \mathbf{w}\mathbf{w} \rangle$ , reaches statistical equilibrium relatively quickly. As a consequence, we may need to solve for the cell problem in  $\tau$  for only a small number of time steps after updating the effective velocity in one coarse grid time step. Moreover, we need not solve the cell problem in every coarse grid for homogeneous flow. It should be sufficient to solve one or a few representative cell problems for fully mixed flow and use the solution of these representative cell solutions to compute the Reynolds stress term in the homogenized velocity equation. If this can be achieved, it would lead to a significant computational saving.

## 5. CONCLUDING REMARKS

Multiscale methods offer several advantages over direct numerical simulations on a fine grid. First, the multiscale bases can be computed locally and independently. This reduces the memory load of multiscale methods and lends them naturally to parallel computation. Secondly, we can use an adaptive strategy to update the multiscale bases only in changing regions, avoiding unnecessary computation. Thirdly, the multiscale methods offer an effective tool in deriving upscaled equations. For example, in oil reservoir simulations, it is often the case that multiple simulations of the same reservoir model must be carried out in order to validate the fine grid reservoir model. After the upscaled model has been obtained, it can be used repeatedly with different boundary conditions and source distributions. In this case, the cost of computing the multiscale base functions is a one-time overhead. If one can coarsen the fine grid by a factor of 10 in each dimension, the computational saving of the upscaled model over the original fine model could be as large as a factor 10 000 (three space dimensions plus time).

It remains a challenge to develop a systematic multiscale analysis to upscale convection-dominated transport in heterogeneous media. There is a need to develop a new type of multiscale analysis which does not require a large separation of scales. One approach is to use the two-scale analysis iteratively and incrementally for problems that have many or continuous spectrum of scales. The dynamic reparameterization technique offers a natural way to implement this strategy. By using dynamic reparameterization, we can always divide a multiscale solution into a large-scale component and a small-scale component. Interaction of the large scales and small scales can be effectively modelled by using a two-scale analysis for short time increments. We then use the reparameterization technique to decompose the solution again into a large-scale component and a small-scale component. Thus, interaction of large- and small-scale solutions occurs iteratively at each small time increment. In this way, over long time intervals, we can account for interactions of all scales. We are currently pursuing this approach with the hope of developing a systematic multiscale analysis for incompressible flow at high Reynolds number.

## ACKNOWLEDGEMENT

This Research was in part supported by a NSF Grant No. ACI-0204932.

## REFERENCES

1. Hou TY, Wu XH. A multiscale finite element method for elliptic problems in composite materials and porous media. *Journal of Computational Physics* 1997; **134**:169–189.
2. Hou TY, Wu XH, Cai Z. Convergence of a multiscale finite element method for elliptic problems with rapidly oscillating coefficients. *Mathematics of Computation* 1999; **68**:913–943.
3. Efendiev YR, Hou TY, Wu XH. Convergence of a nonconforming multiscale finite element method. *SIAM Journal on Numerical Analysis* 2000; **37**:888–910.
4. Chen Z, Hou TY. A mixed finite element method for elliptic problems with rapidly oscillating coefficients. *Mathematics of Computation* 2002; **72**:541–576.
5. Babuska I, Caloz G, Osborn EJ. Special finite element methods for a class of second order elliptic problems with rough coefficients. *SIAM Journal on Numerical Analysis* 1994; **31**:945–981.
6. Brezzi F, Russo A. Choosing bubbles for advection–diffusion problems. *Mathematical Models and Methods in the Applied Sciences* 1994; **4**:571–587.
7. Hughes T. Multiscale phenomena: Green’s functions, the Dirichlet-to-Neumann formulation, subgrid scale models, bubbles and the origins of stabilized methods. *Computer Methods in Applied Mechanics and Engineering* 1995; **127**:387–401.

8. Smith EH. The influence of small-scale heterogeneity on average relative permeability. In *Reservoir Characterization II*, Lake LW, Carroll Jr HB, Wasson TC (eds). Academic: New York, 1991; 52–76.
9. Warren JE, Price HS. Flow in heterogeneous porous media. *Society of Petroleum Engineers Journal* 1961; 153–169.
10. Bensoussan A, Lions JL, Papanicolaou G. *Asymptotic Analysis for Periodic Structures* (1st edn). North-Holland: Amsterdam, 1978.
11. Tartar T. Nonlocal effects induced by homogenization. In *PDE and Calculus of Variations*, Culumбини F *et al.* (eds). Birkhäuser: Boston, 1989; 925–938.
12. Efendiev YR, Durlofsky LJ, Lee SH. Modeling of subgrid effects in coarse-scale simulations of transport in heterogeneous porous media. *Water Resources Research* 2000; **36**:2031–2041.
13. Jenny P, Lee SH, Tchelepi H. Adaptive multi-scale finite volume method for multi-phase flow and transport in porous media. *Multiscale Modeling and Simulation* 2005; **3**(1):50–64.
14. Hou TY, Westhead A, Yang D. Multiscale analysis and computation for two-phase flows in strongly heterogeneous porous media. 2004, in preparation.
15. Wallstrom T, Hou S, Christie MA, Durlofsky LJ, Sharp D. Accurate scale up of two-phase flow using renormalization and nonuniform coarsening. *Computational Geoscience* 1999; **3**:69–87.
16. Arbogast T. Numerical subgrid upscaling of two-phase flow in porous media. In *Numerical Treatment of Multiphase Flows in Porous Media*, Chen Z *et al.* (eds). Springer: Berlin, 2000; 35–49.
17. Matache AM, Babuska I, Schwab C. Generalized p-FEM in homogenization. *Numerische Mathematik* 2000; **86**:319–375.
18. Cao LQ, Cui JZ, Zhu DC. Multiscale asymptotic analysis and numerical simulation for the second order Helmholtz equations with rapidly oscillating coefficients. *SIAM Journal on Numerical Analysis* 2002; **40**: 543–577.
19. Weinan E, Engquist B. The heterogeneous multi-scale methods. *Communications in Mathematical Science* 2003; **1**(1):87–133.
20. Smogorinsky J. General circulation experiments with the primitive equations. *Monthly Weather Review* 1963; **91**:99–164.
21. Germano M, Pimomelli U, Moin P, Cabot W. A dynamic subgrid-scale eddy viscosity model. *Physics of Fluids A* 1991; **3**:1760–1765.
22. McLaughlin DW, Papanicolaou GC, Pironneau O. Convection of microstructure and related problems *SIAM Journal on Applied Mathematics* 1985; **45**:780–797.
23. Hou TY, Yang D, Wang K. Homogenization of incompressible Euler equations. *Journal of Computational Mathematics* 2004; **22**(2):220–229.